THE CONSTRUCTION OF A 200 keV ELECTROSTATIC ACCELERATOR

By

Peter T. Brady

A thesis submitted in partial fulfillment of the
requirements for the degree of

Bachelor of Science

Houghton College

April 2004

Signature of Author……………………………………………………………………..

Department of Physics
April 30, 2004

………………………………………………………………………………………..

Dr. Mark Yuly
Professor of Physics
Research Supervisor

………………………………………………………………………………………..

Dr. Ronald Rohe
Associate Professor of Physics

THE CONSTRUCTION OF A 200 keV ELECTROSTATIC ACCELERATOR

By

Peter T. Brady

Submitted to the Department of Physics
on April 30, 2004 in partial fulfillment of the
requirement for the degree of
Bachelor of Science

Abstract

The original 200 keV electrostatic electron accelerator at Houghton College used a glass acceleration tube with external copper equipotential rings to provide the required uniform electric field along the length of the tube. Unfortunately, in this design stray electrons striking the walls of the tube caused charge to accumulate on the inside wall, eventually deflecting the electron beam. In order to solve this problem, a new design for the acceleration tube is being tested, made up of 51 pairs of alternating aluminum and plastic rings, with inside diameters 3.8 cm and 5.1 cm respectively. The differing inner radii of the rings ensure that the electrons will only strike the aluminum rings, and can therefore be removed as part of the coronal current flowing down the exterior column.

Thesis Supervisor: Dr. Mark Yuly
Title: Professor of Physics

TABLE OF CONTENTS

TABLE OF FIGURES

Chapter 1

INTRODUCTION

The particle accelerator has proven to be a very powerful tool in modern physics. Nuclear structure and nuclear interactions can be studied with the high energy beams of particles produced by accelerators. Therefore, a small 200 keV electrostatic accelerator has been constructed at Houghton College. This accelerator can be used for low energy scattering experiments using an electron gun to create electron beams of approximately 200 keV. The bremsstrahlung x-rays produced by the electrons striking a target can also be used for experiments. By using a positive ion source, experiments can be performed with beams of ions, and positive ion beams can be used to create neutron beams for neutron scattering and absorption experiments.

1.1 What is an Electrostatic Accelerator?

An electrostatic accelerator is a type of accelerator that uses a static electric field to accelerate charged particles. There are four main components to an electrostatic accelerator, as shown in Figure 1. For an electron accelerator the high voltage source is used to create a large potential difference between the anode and the high voltage terminal. An electron gun is positioned inside the high voltage terminal and injects electrons into the accelerating tube. Within the accelerating tube is a strong uniform electric field which accelerates electrons toward the anode. The vacuum system lowers the pressure of the accelerating tube down to at least 10^{-5} Torr to ensure that the electrons being accelerated will not interact with air molecules and lose energy.

1.2 History and Motivation

Lord Kelvin proposed the first electrostatic generator with his charged water drop generator. In this device, water drops are squeezed from a nozzle and electrified by friction. The drops fall and accumulate in an insulated metal container, raising it to a high potential [1]. There are many

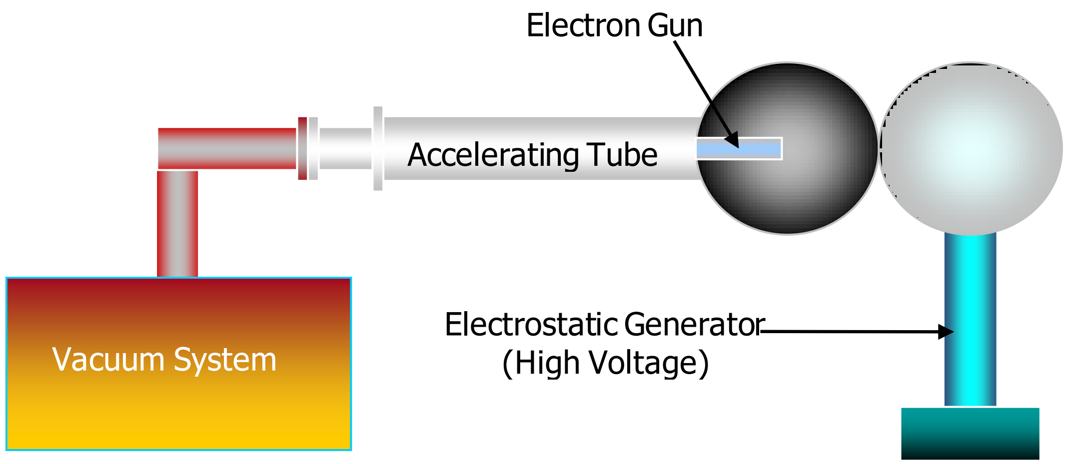

Figure 1. A simplified schematic of an electrostatic electron accelerator showing the four main parts: the high voltage source, electron gun, accelerating tube, and vacuum system.

methods for accumulating charge that are modifications of Kelvin's first generator. One method, for example, is to spray ionized dust down an insulating tube [2]. Another method, which was pioneered by Righi [1] is the use of a motor driven belt to carry charge. Charge is sprayed onto the belt, which is driven by a motor to carry the charge up into a conducting sphere where it is deposited. The belt is enclosed by an insulated column which supports the conducting sphere. One use for these types of generators is to provide the high voltages needed to directly accelerate particles to disintegrate nuclei.

In 1919 Earnest Rutherford used alpha particles from naturally radioactive radium and thorium to achieve the first artificial disintegration of a nucleus [3] ($^{14}_{7}N+^{4}_{2}\alpha\rightarrow^{1}_{1}H+^{17}_{8}O$). This opened up the previously hidden world of the nucleus to be studied in depth by physicists. Physicists began to build machines to study nuclear interactions as Rutherford urged in 1927 before the Royal Society [4]. These machines, later called particle accelerators, are better suited to the study of nuclear interactions than radioactive sources because the radiation may be easily and turned on and off at will whereas a radioactive source is always "on" and must therefore be handled with care. Also, the energy of the particles may be controlled with an accelerator. Particle accelerators can also to be used to collide a wide variety of particles. For example, at Brookhaven National Laboratory, two beams of 200 GeV gold nuclei are collided with each other. There is no way these 200 GeV gold nuclei may be obtained from radioactive sources.

One type of machine used to generate high voltage was the Tesla coil. A Tesla coil is a resonance transformer which uses electromagnetic induction to develop oscillating pulses of large potential [5]. These were investigated as high voltage sources for charged particle acceleration at the Carnegie Institution of Washington in 1930 [5,6]. Potentials as high as 5 MV were reported, but are not believed to be accurate [1]. During these experiments it was found that evacuated glass tubes break down around 300 KV. Charge accumulated on the walls of the tube creating punctures and even making the tube a conductor, short circuiting the high voltage power source. To remedy this problem, tubes of alternating insulating and conducting regions, known as Coolidge or cascade tubes, were developed [6,7]. Increasing the number of electrodes enabled these tubes to handle higher voltages. However, the rapidly oscillating nature of the Tesla coil made it unsuitable for use as a particle accelerator and the group eventually abandoned it in favor of R. J. Van de Graaff's electrostatic generator.

Another method for generating high voltages developed is the voltage multiplier circuit. A voltage multiplier is a capacitor-rectifier circuit set up so the input voltage is multiplied by the number of capacitors in the circuit. This is done by charging the capacitors in parallel and discharging them in series [1]. J.D. Cockroft and E.T.S. Walton used a voltage multiplier in 1932 to produce 400 keV protons which were used to study the nuclear disintegration of lithium [8]. Cockroft and Walton were the first to achieve nuclear disintegration using artificially accelerated particles, but due to problems associated with damage to their accelerating tube from sparks, Van de Graaff generators became more popular.

Van de Graaff is famous for his belt charged generator, which he built in 1929 [9]. Charges were sprayed onto a silk belt which transported them through a 7 foot long glass tube to a 2 foot diameter aluminum sphere as shown Figure 2. The initial success of this type of charging system over other forms of electrostatic generators prompted Van de Graaff, K.T. Compton, and L.C. Van Atta to construct two such generators with spheres 15 feet in diameter [10] as seen in Figure 3. One sphere generated a positive voltage of 2.4 MV, the other a negative voltage of 2.7 MV [11]. An accelerating tube was mounted between the two for the purpose of accelerating ions. Due to the difficulties in evacuating and mounting the accelerating tube, as well as the relatively high humidity of the area, the theoretical 10 MV potential difference was never achieved.

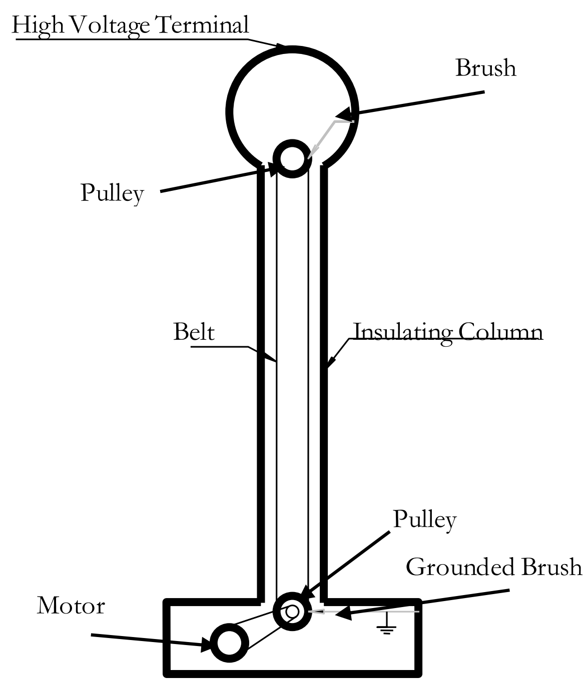

Figure 2. A drawing of Van de Graaff's 7ft tall generator. Charge is sprayed onto the belt and carried by a motor driven pulley into the spherical high voltage terminal where it is deposited.

Van de Graaff's belt charged generators proved to be better than most of the early competitors for a number of reasons. Because of the remarkably steady high voltage they were able to produce beams of constant energy, which is very important since the probability of a reaction depends mainly on incident energy [12]. They were also better suited to beam focusing, and allowed the potentials to be measured more accurately than a.c. generators [10].

Figure 3. Large generators at Round Hill. They are 15 feet in diameter and generated a potential difference of 5.1 MV. The building is 140 ft tall. Taken from reference [13].

As can be seen in Figure 4, which shows the energy of particle accelerators plotted against years, the real competition with Van de Graaff's electrostatic generator was the cyclotron. Rather than using high voltages, the cyclotron accelerates heavy charged particles to high energies by apply an oscillating electric field to two electrodes at the resonant frequency of the particles in the presence of a uniform magnetic field. The cyclotron is therefore not limited by accelerating tube breakdown voltages and coronal discharge as electrostatic generators are. In 1932 Ernest Lawrence and M. Livingston used their cyclotron to produce 1 MeV protons [14]. This was the first time artificially accelerated particles of this energy were produced.

Belt charged electrostatic generators reached their peak energy of about 10-15 MV in the 1940's as shown in Figure 4, and were surpassed by larger and higher energy accelerators such as the cyclotron, betatron, synchrocyclotron, and synchrotron. The Tevatron at Fermilab, currently the

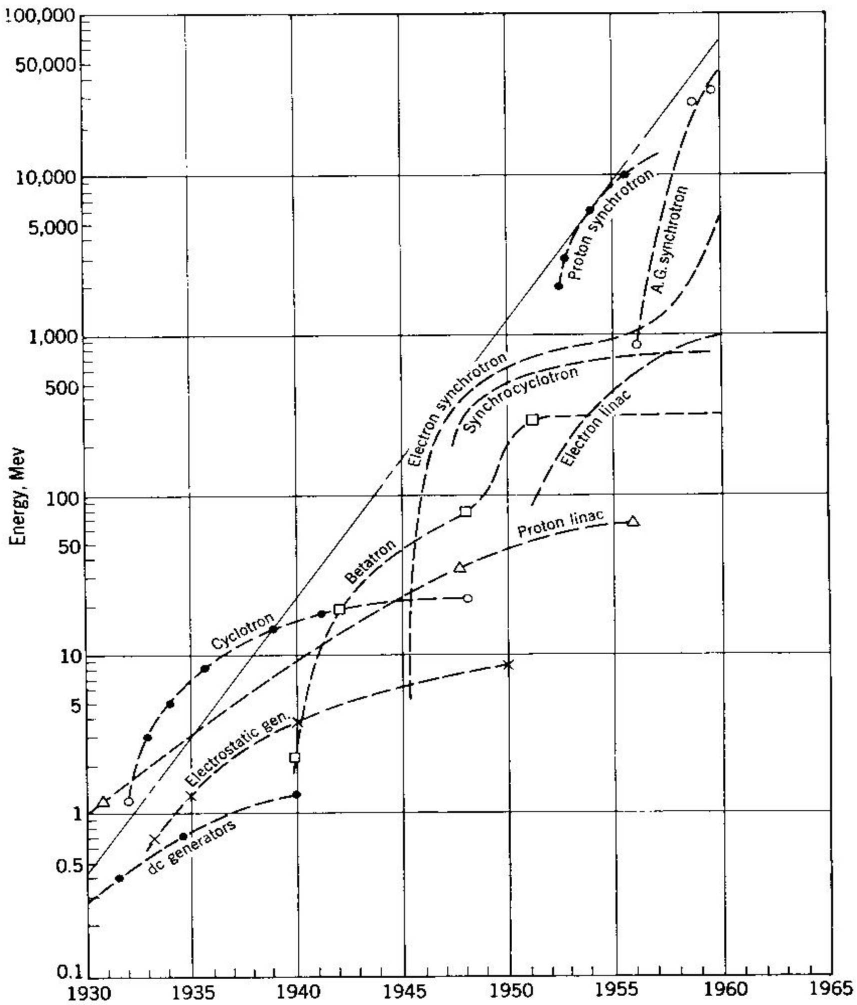

Figure 4. This a graph showing the energy of particle accelerators plotted against the years of their main use. The cyclotron was developed around the same time as electrostatic generator and is, in general, capable of higher energies. Taken from reference [1].

the highest energy accelerator in the world, has a 4 mile circumference, and proton beam energy of 980 GeV [15]. In big laboratories today, such as the Brookhaven National Laboratory, electrostatic generators are used as injectors, accelerating particles into more powerful accelerators. But this does not mean that every valuable experiment at lower energies has been performed.

The relatively low cost of building a low-energy electrostatic accelerator and the possibility of using it to do original research has made it a favorite of amateur scientists. F.B. Lee, a chemical engineer, built an electrostatic accelerator [16] mostly from scrap parts in 1959. The accelerating tube was a three foot long pyrex tube. The high voltage was supplied by a purchased Van de Graaff generator. Copper wire wound into rings around the pyrex tube at even intervals provided a uniform electric field. The most expensive part of the project would have been the vacuum pumps, so these were built from old refrigerator compressors. Larry Cress built a similar type of accelerator, and constructed the pressure gauges as well [17]. The accelerator he constructed was used mainly to accelerate deuterium. Fred M. Niell, a high school student at the time, built an accelerator in 1992 using a twenty stage Cockroft Walton voltage multiplier to supply 100 kV [18]. The vacuum system and detectors were homemade or donated by schools and hospitals.

1.3 The Houghton College Electrostatic Accelerator

The Houghton College electrostatic accelerator utilizes a Van de Graaff generator to supply approximately 200 kV, depending on the belt speed. The spherical high voltage terminal of the Van de Graaff generator is brought into electrical contact with another spherical terminal inside of which is an electron gun attached to the accelerating tube. Electrons from the cathode are then accelerated from the high voltage terminal to the grounded end of the accelerating tube where a Faraday cup is placed to measure the beam current.

The preliminary design (see Ref. 19) used a glass accelerating tube 110.7 cm in length and 3.8 cm in diameter with copper wire wound into rings around the glass at even intervals (as shown in Figure 5) to provide a uniform electric field.

This design had two main problems. Electrons from the cathode (or discharges near the cathode) would strike the inside of the glass tube. Eventually enough charge accumulated on the glass to deflect the electron beam. When the high voltage was applied electric discharges occurred often, which ionized the residual gas in the accelerating tube, and produced a wildly fluctuating beam

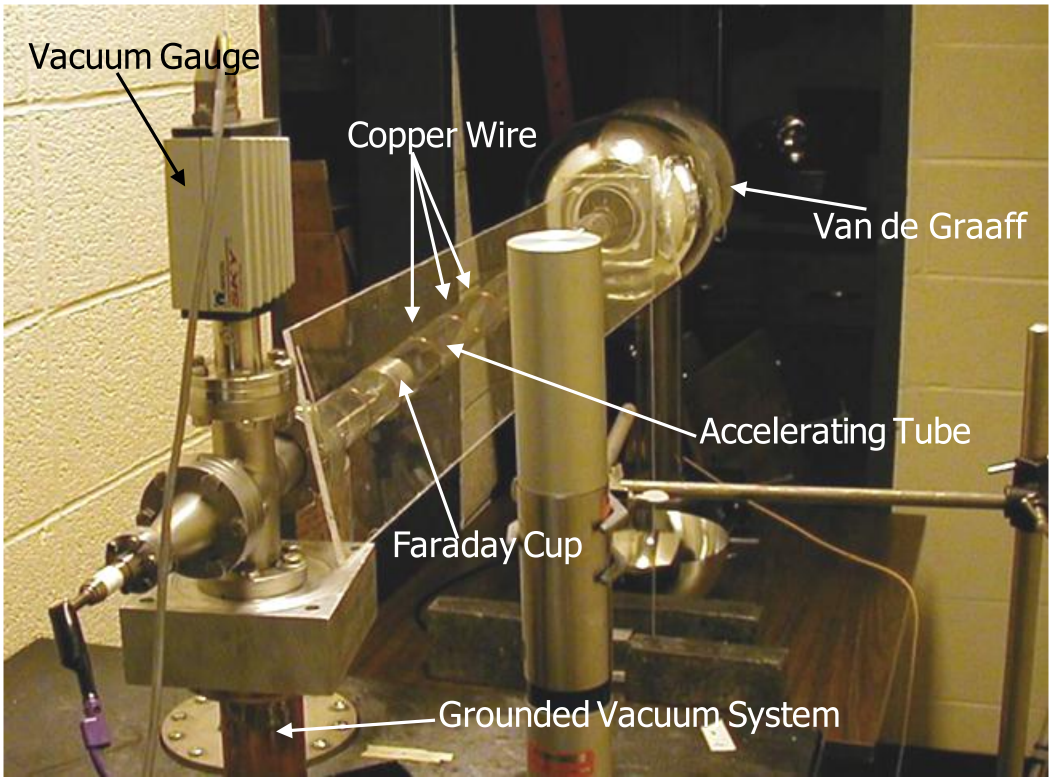

Figure 5: A photograph of the preliminary setup. The Van de Graaff generator and high voltage terminal are at the far end of the glass tube. The faraday cup is visible inside the glass tube at the opposite the high voltage terminal. A dual ion/piranni gauge attached to the top flange was used to measure pressure. The scintillator held in the ring clamp was placed at various angles to measure bremsstrahlung x-ray energy spectra.

current even when the filament was off. When the electrons from the ionized gas were accelerated down the tube, x-rays were produced on collision with the Faraday cup and the bremsstrahlung x-ray energy spectrum was measured even with the filament off.

To solve these problems a new accelerating tube was constructed which consists of 51 alternating aluminum and high density polyethylene rings, as shown in Figure 6. The high density polyethylene rings have a larger inner radius then the aluminum rings to ensure that electrons can only strike the aluminum rings, so they will then become part of the coronal current flowing down the outside of the accelerating column.

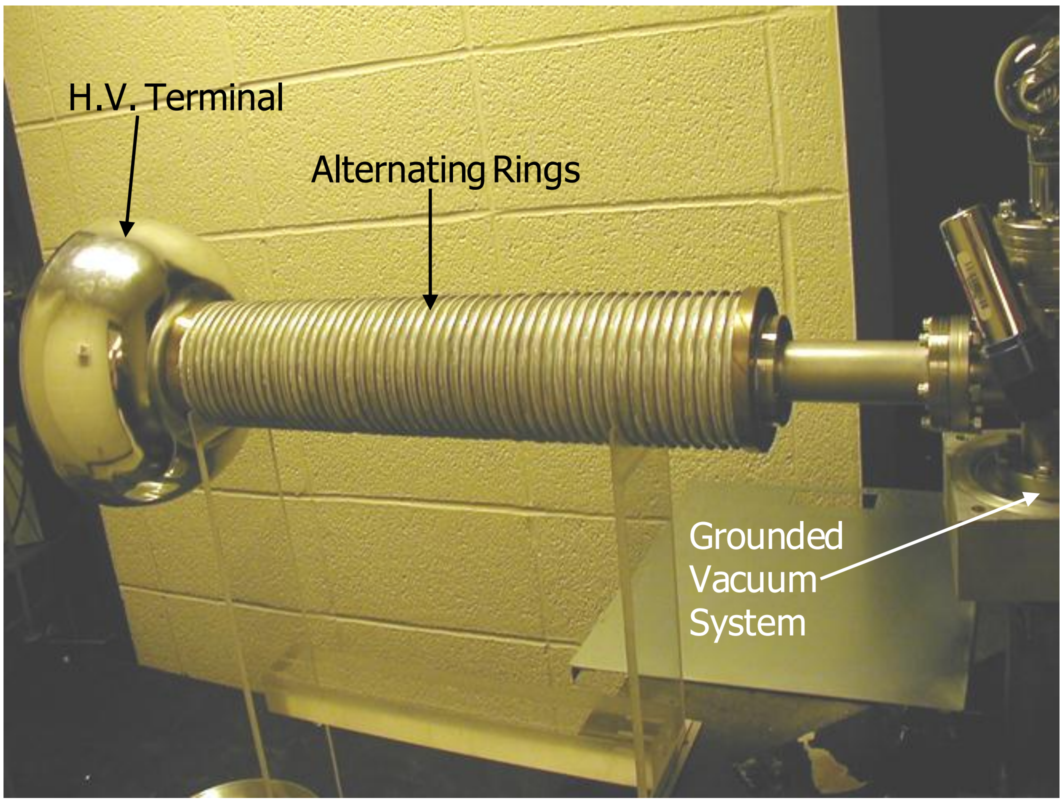

Figure 6. A photograph of the new accelerating tube made of alternating aluminum and high density polyethylene rings. The aluminum rings are the slightly larger gray rings.

Chapter 2

THEORY OF OPERATION

In this chapter the theory of operation for the Van de Graaff generator, electron gun, and accelerating tube will be discussed. The simulations used to model the operation of the accelerator will also be discribed.

2.1 Van De Graaff Generator

The Van De Graaff generator is a made up of an insulating belt, an insulating column which contains the belt, and a conducting "sphere" which rests on top of the insulating column as shown in Figure 2. The motor causes the bottom pulley rotate, which causes the belt to move. As the bottom pulley and belt rotate, they rub against each other, and due to the difference in the electronegativity of the two materials, electrons are pulled from the pulley onto the belt leaving the pulley positively charged. Electrons from the grounded wire brush are attracted to the positively charged pulley and are sprayed onto the belt which is between the pulley and the grounded wire brush. The belt carries the charge into the conducting sphere where it is removed by another wire brush connected to the high voltage terminal. Charge is deposited on the surface of the sphere because all charge in a conductor resides on the surface.

The spherical high voltage terminal behaves like a spherical capacitor, which has capacitance

$$C = 4\pi\varepsilon_0 r \tag{1}$$

where r is the radius of the high voltage terminal. Therefore the voltage V of the sphere is determined by the charge on it:

$$Q = CV \, . \tag{2}$$

Some factors that limit the maximum potential obtained with a Van de Graaff are the current that travels down the insulating column and the coronal discharge into the air. At low potentials this is very small but in the presence of strong electric fields (which accompany potentials of a few hundred kilovolts) this effect is large. When an accelerating tube is attached to the Van de Graaff generator the current that travels down the accelerating tube and the beam current also lower the maximum potential. After a while the terminal will reach an equilibrium potential where the charge delivered by the belt is equal to the charge leaving the terminal [20].

From differentiating equation (2), the potential increases as:

$$\frac{dV}{dt} = \frac{i}{C} \tag{3}$$

where i is the current flowing to the capacitor. The current i consists of the up current (charge brought to the high voltage terminal by the belt) and the down current (charge that bleeds off the high voltage terminal). The up current a is a constant determined solely by the belt speed while the down current b, using Ohm's law varies linearly with V:

$$b = \frac{V}{\lambda} \tag{4}$$

where λ is the "resistance" between the high voltage terminal and ground. There are probably non-linear components as well, but these will be considered negligible. Rewriting the current i as the sum of the up current and down current,

$$\frac{dV}{dt} = \frac{a}{C} - \frac{V}{\lambda C}\,. \tag{5}$$

The solution to differential equation (5) is

$$V = a\lambda\left(1 - \exp\left(-\frac{t}{\lambda C}\right)\right). \tag{6}$$

Observe that at t = 0, the potential is zero. As time progresses the potential of the high voltage approaches the value $a\lambda$. Therefore the maximum voltage of the terminal can be increased by increasing either the up current (belt speed) or increasing the terminal's "resistance" to ground. In most instances the latter is accomplished by encasing the Van de Graaff in high pressure container (usually nitrogen).

As with all capacitors one of the limiting factors for the potential obtained with a Van de Graaff generator is the breakdown of the dielectric medium (in this case air) between the high voltage terminal and ground. The dielectric strength of air at standard temperature and pressure and negligible humidity about *3 MV/m*.

The magnitude of the electric field due to a sphere of charge Q is

$$E = \frac{1}{4\pi\varepsilon_0}\frac{Q}{r^2} \tag{7}$$

where r is the distance from the center of the sphere. Using equation (1) and (2) to substitute for Q, the magnitude of the electric field at the surface of the high voltage terminal is

$$E = \frac{V}{r}. \tag{8}$$

The maximum E is the dielectric strength of air, and the radius of the high voltage terminal is 12.5 cm, so the maximum potential obtainable with the high voltage terminal is

$$V_{max} = 375{,}000\ \mathrm{V} \tag{9}$$

Using equation (1) , (2) and (9) to solve for the maximum charge yields the maximum charge on the high voltage terminal

$$Q_{max} = 5.2\ \mu\text{C}. \tag{10}$$

If Q is the charge of the high voltage terminal then there is an electrostatic repulsion between the terminal and the electrons on the belt being transported to the terminal given by Coulomb's law:

$$F = \frac{1}{4\pi\varepsilon_0}\frac{Qe}{r^2} \tag{11}$$

where r is distance between the center of the sphere and the electron. Therefore the motor must do work to transport the charges into the sphere. This work is stored in the high voltage terminal as potential energy with a magnitude

$$U = \frac{1}{2}CV^2. \tag{12}$$

If it were possible to achieve V_{max} then

$$U_{max} = 0.98\ \text{J} \tag{13}$$

2.2 Accelerating Tube

The accelerating tube was designed to provide an electric field parallel to the tube axis to accelerate electrons from the high voltage terminal to the grounded end of the acceleration tube. The tube is made up of 51 alternating, equally spaced aluminum and high density polyethylene rings. At high voltages it behaves as a voltage divider as shown in Figure 7, with the resistances a function of the distance between the rings and voltage V and therefore all the same. Since the current flowing down the column approximately flows through each ring, by Ohm's law there will be a constant voltage drop across each ring.

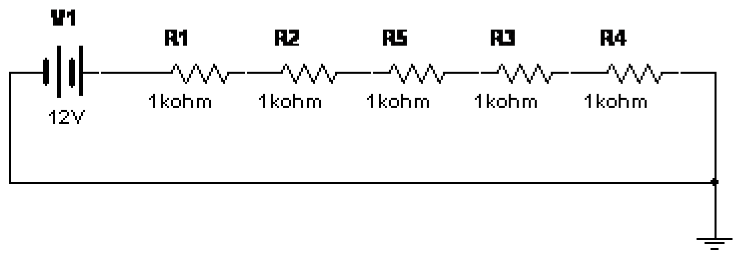

Figure 7. Circuit diagram of a voltage divider. A current I flows from the power supply to ground. By Ohm's law there is a voltage drop of IR across a resistor R.

The electric field $\vec{E}$ is given by $\vec{E} = -\vec{\nabla}V$ where V is the potential. It is clear then that a uniform drop in potential results in a constant $\vec{E}$ field of magnitude V/L where L is the length of the accelerating tube. A constant voltage drop produces and electric field with the field lines running parallel to the axis of the accelerating tube. If the voltage was drop was not constant the electric field lines would bend, accelerating particles in undesirable directions. Combining the Lorentz force with Newton's second law yields an electron acceleration of magnitude $a = eV/Lm_e$ where e is the charge of the electron and m_e is the mass of the electron.

In order to determine the maximum potential held by each ring before a discharge would occur, measurements were made using square sheets of aluminum of side 20.32 cm separated by a sheet of high density polyethylene of thickness of 1.27 cm, which were able to maintain a potential difference of approximately 7 kV before sparking. Based on these results it was concluded that a potential difference of approximately 5 kV could be applied to neighboring aluminum rings without the risk of electric discharge between them. The accelerating tube is split up into 51 conducting regions and can therefore theoretically maintain a potential difference of approximately 250 keV.

2.3 Electron Gun

The electron gun is located inside the high voltage terminal and injects electrons into the accelerating tube. The preliminary electron gun was a filament, cathode, and control grid as shown in Figure 8. The cathode is from an old RCA 3RP1 cathode ray tube. Current through the filament caused it to heat up the cathode, which is a metal coated with a material having a low work function which releases electrons relatively easily. The electrons have energies on the order of kT (where $k = 8.62 \times 10^{-5}\,\mathrm{eV/K}$ is Boltzmann's constant). A typical filament temperature is 2,250 K, making kT approximately 0.2 eV with a spread of energies described by the Maxwell-Boltzmann energy distribution. The control grid is biased according to the desired beam intensity. A negatively biased control grid reduces the intensity of the beam by only allowing electrons with energies above a certain threshold to pass. A positively biased control grid will allow all electrons to pass.

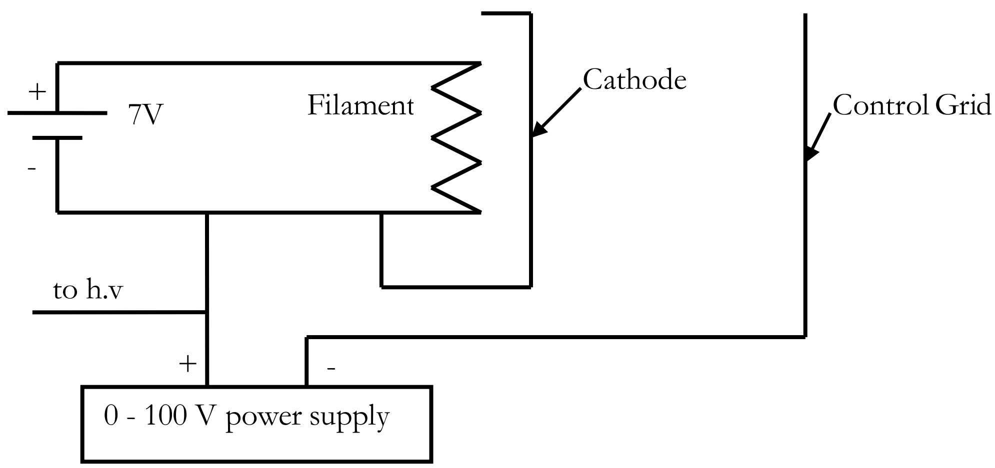

Figure 8. A schematic of the preliminary electron gun with the filament, cathode, and control grid labeled with the biasing used. Electrons are boiled off the cathode and repelled by the control grid.

2.4 Simulations

To verify that the accelerator would actually accelerate electrons toward the grounded end of the accelerating tube, simulations were run using Simion 3D v7.0 to study focusing and determine the position of the cathode which yielded the smallest beam spot. The simulations were also helpful in determining the proper biasing of the electron gun.

To operate Simion, the locations and sizes of the electrodes were input with their proper potentials. Simion then used these potentials as boundary values to solve Laplace's equation to determine the potential everywhere. The program approximates solutions to Laplace's equation with a finite difference technique called over-relaxation, which is based on successive approximations [21]. In each iteration the potential of a point is estimated based on the fields of the four nearest points. For a 3D simulation the 6 nearest neighbors are used. As the iterations proceed, the potentials change less and less with each iteration. Simion takes the values of the potential as an approximate solution to Laplace's equation when this change is less than a certain value.

Simion estimates the potential of four points that are 0.5 grid units away from the ion. These points are then used to determine the voltage gradient and hence electric field at the ions position.

A simulation of the accelerator with the preliminary electron gun is shown in Figure 9. Observe that the electron gun is only a cathode and approximately 1/8 of the electrons make it to the accelerating tube. Due to the size of our apparatus, Simion was only able to model coaxial symmetry so the effect of a lopsided ring on the accelerating tube is unknown

Experimentally, this set up failed to produce any beam current. The problem was believed to be that the cathode, which is located approximately 10.2 cm behind the entrance of high voltage terminal as shown in Figure 10, was too far back in the zero electric field region for the 0.2 eV electrons to make it to the accelerating tube. To solve this problem the electron gun was modified by adding an accelerating grid as shown in Figure 11. The control grid and accelerating grid were positively biased to draw electrons being released from the cathode toward the accelerating tube. The biasing of the grids were chosen and then verified with Simion.

Simion simulations of the accelerator with the modified electron gun are shown in Figure 12. Observe that a much larger fraction of the electrons are injected into the accelerating tube with the modified electron gun. As will be discussed in chapter 4, a beam current was measured experimentally with this set up.

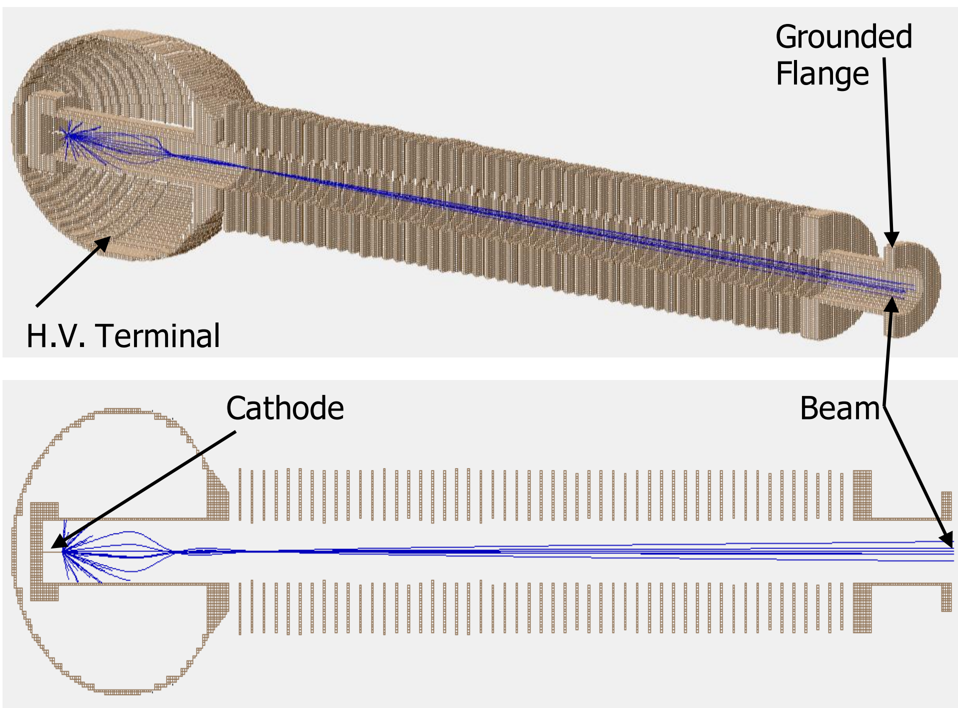

Figure 9. Simion 7.0 simulation of the acclerator with the preliminary electron gun. Some of the rings are different sizes to model slight asymmetries in the actual accelerator. The high voltage terminal is not to scale due to computer memory limitations.

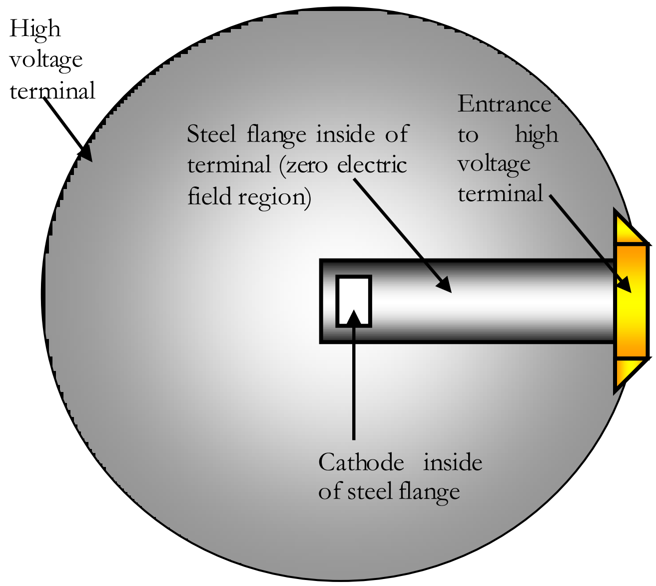

Figure 10. Simplified drawing of the cathode inside the high voltage terminal. The cathode is in a zero electric field region 10.2 cm behind the entrance to the high voltage terminal.

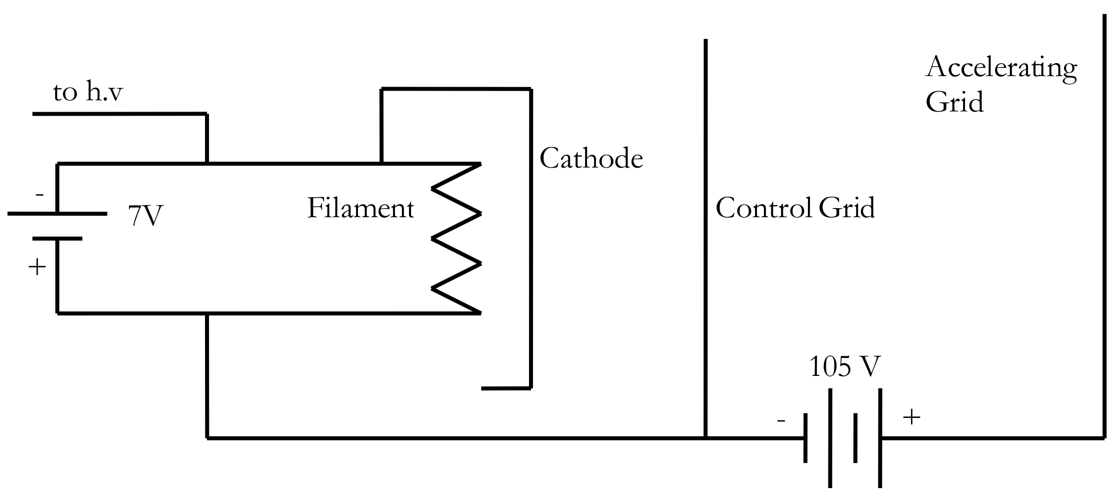

Figure 11. Circuit diagram of modified electron gun with biasing shown. The control grid and accelerating grid are forward biased to inject electrons into the accelerator.

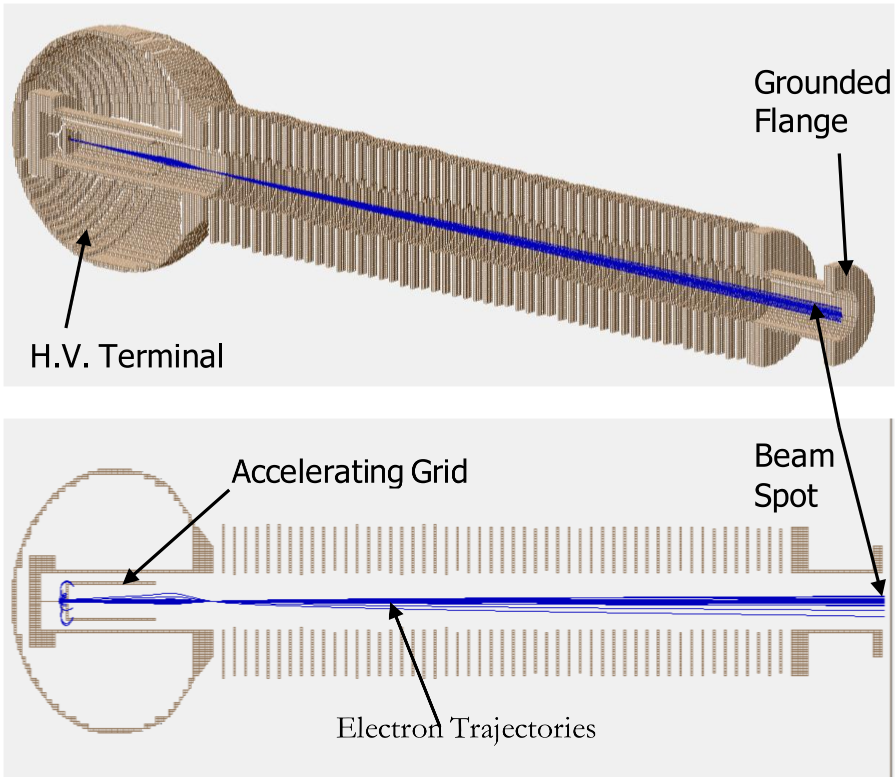

Figure 12. Simion 7.0 simulation of the accelerator with the modified electron gun. The high voltage terminal is not to scale due to computer memory limitations.

.

Chapter 3

CONSTRUCTION

A detailed description of the construction of the accelerating tube will be given in this chapter. This will include how the rings were made and epoxied together, as well the flanges used and the manner in which the high voltage terminal was attached to the accelerator. The location of the power supply for the electron gun will also be described.

3.1 Rings

The new accelerating tube consists of 51 alternating 5052 aluminum rings and high density polyethylene rings, 0.3 cm thick and 0.6 cm thick, respectively, with dimensions shown in Figure 13. The rings were cut on a Microkinetics CNC "Benchtop Mill" using a computer program, Millmaster Pro for Dos v. 1.7. This was done to ensure that all the rings were indentical, and that the four smaller holes would be aligned on all the rings. The diameter of the aluminum ring is 10.16 cm because that is the maximum range of motion of the milling machine bed.

3.2 Accelerating Tube

To assemble the accelerating tube, after all the rings had been cut out, the region between the inner radius and the four smaller holes was roughened with fine emery cloth on each ring to provide a stronger bond with Hysol Epoxi-Patch EPK 1C. A high density polyethylene ring was laid flat on a level table and held down while 0.65 cm delrin rods were placed in the four smaller holes forming a very tight fit. In fact, the fit was so tight that the holes had to be reamed out (with a reamer) slightly for the rings to be able to slide down the rods. The delrin rods were then fit in the four smaller holes of an aluminim ring which was pushed down the length of the rods until it was approximately 10 cm above the bottom high density polyethylene ring. A level was placed on top of the aluminum ring to make sure the structure was level. The delrin rods were then fit in to the four smaller holes of another high density polyethylene ring which was slid down the rods until it made contact with the aluminum ring. This process was repeated until all 103 rings were on the delrin rods, with the bottom ring being separated from the next aluminum ring by about 10 cm. This was done to ensure that all the rings would remain aligned on the now very sturdy and vertical delrin rods during the gluing process. A level was used after every 5 rings were placed on the rods to make sure the structure remained level.

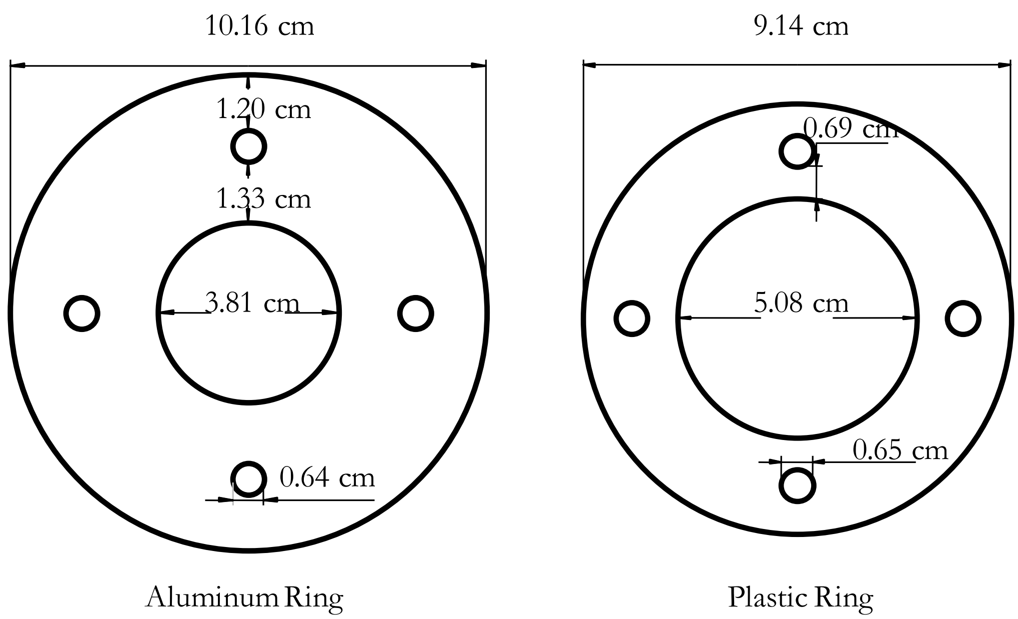

Figure 13. Drawings of the aluminum and high density polyethylene rings used in the construction of the new accelerating tube.

The faces of the bottom high density polyethylene ring and the aluminum ring above it were cleaned with isopropyl alcohol and then epoxy was applied to the roughened regions on the bottom ring with a wooden applicator. The aluminum ring was then pushed down until good contact was made with the bottom ring. The structure was then checked with a level before the epoxy cured. This process was repeated until all the rings had been epoxied. The inside of the high density polyethylene rings were coated with the epoxy as the rings were glued together to reduce out gassing from the plastic since the vapor pressure of the epoxy is around 10^{-8} Torr. It was later discovered, however, that this precaution was not enough to stop the accelerating tube from leaking. To stop the leaks, all the outside joints were later also coated with epoxy.

Sharp edges generate high electric fields which will cause electric discharges, so the inner edges on the aluminum rings were smoothed with a reamer. The rings were then spun on a lathe and sanded with medium emery cloth until the outer edges were smooth.

Flanges of C9504 aluminum-bronze were made to attach the accelerating tube to the vacuum system and the feed through flange for the cathode in the high voltage terminal. The flange at the grounded end has a width of 1.3 cm and a diameter of 10.3 cm. The flange attached to the HV side was cut at an angle to reduce the chance of accidental electric discharge. The width of this flange is 1.3 cm and the face epoxied to the high density polyethylene ring has a diameter of 9.1 cm while the face attached to the high voltage terminal has diameter of 10.2 cm. 6.985 cm (2.75") conflat 304 stainless steel full nipples 12.7 cm long with one rotatable end were glued with vacuum epoxy to the aluminum-bronze flanges which had previously been attached to the accelerating tube (as shown in Figure 14). Viton O-rings were used to attach the accelerating tube to the vacuum system and cathode feed through flange.

To attach the high voltage terminal to the accelerating tube four holes for 8-32 screws were drilled and tapped in the larger face of the aluminum bronze flange. The high voltage terminal was held in place while a sheet of aluminum was screwed to the flange, pinching the high voltage terminal between the flange and the sheet, thereby holding it in place.

With the high voltage terminal and the feed through flange for the cathode in place, the batteries could to be set up. The 6.3 V filament required 5 C-cell batteries and the bias for the accelerating grid required eleven 9-V batteries connected in series. The 9-V batteries were attached to a small sheet of plastic with tape, then placed inside the high voltage terminal. The C-cell batteries were placed on top of the 9-V batteries. The high voltage terminal acts like a faraday cage, so the batteries were unaffected by the large electric field outside the terminal.

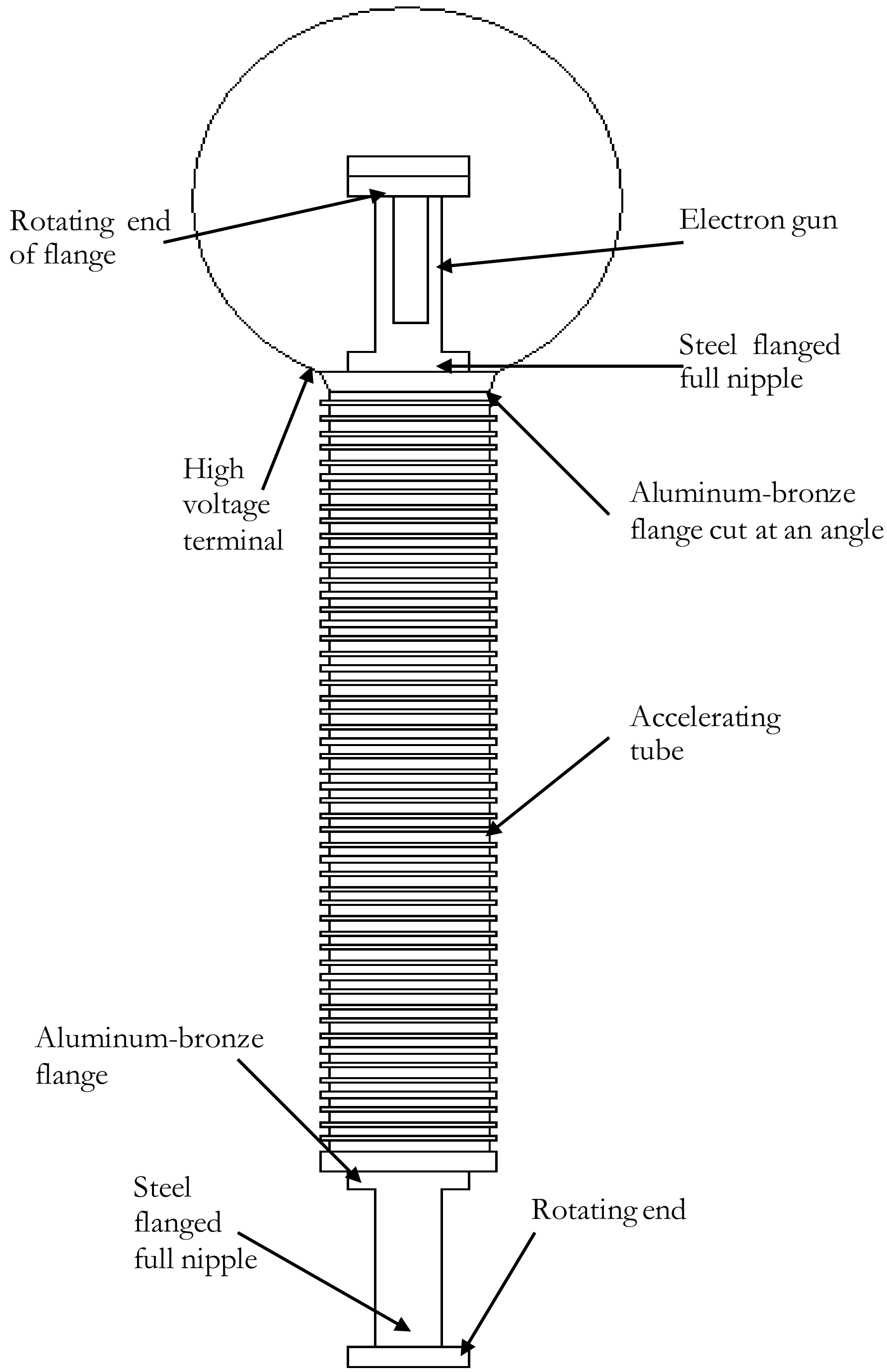

Figure 14. Drawing of the accelerating tube. Stainless steel full nipples are attached to aluminum-bronze flanges. The aluminum bronze flange attached to the high voltage terminal is cut at an angle.

Chapter 4

EXPERIMENT

After the accelerating tube was constructed and attached to the vacuum system and high voltage terminal the accelerator was ready to be tested. In this chapter the experimental results of the trial run of accelerator will be described, such as the measurement of the bremsstrahlung x-ray energy spectra and radiation dosage rates.

4.1 Experimental Setup

The experimental setup is shown in Figure 15. The Van de Graaff generator is in contact with the high voltage terminal, inside of which is the electron gun. The electron gun injects electrons into the accelerating tube. The electrons are accelerated down the accelerating tube toward the grounded Faraday cup which is connected to ground through a microammeter to allow the measurement of beam current. The Faraday cup is an aluminum cylinder that contains a phosphorescent powder which scintillates when struck by electrons, permitting the observation of the beam spot.

4.2 Modified Electron Gun

As discussed in the theory section, the original electron gun was modified by adding an accelerating grid and biasing it +105 V higher than the cathode. The accelerating grid, as shown in Figure 16, is a 7.6 cm long copper pipe with a 1.3 cm diameter. A 0.32 cm hole was drilled in the front cap. The copper pipe was placed approximately 0.2 cm in front of the control grid. With this new design the 0.2 eV electrons immediately receive an approximately 7 eV boost from the control grid, followed by a 100 eV boost from the accelerating grid, to inject them into the accelerator. A beam spot was observed and a beam current was measured using the modified electron gun.

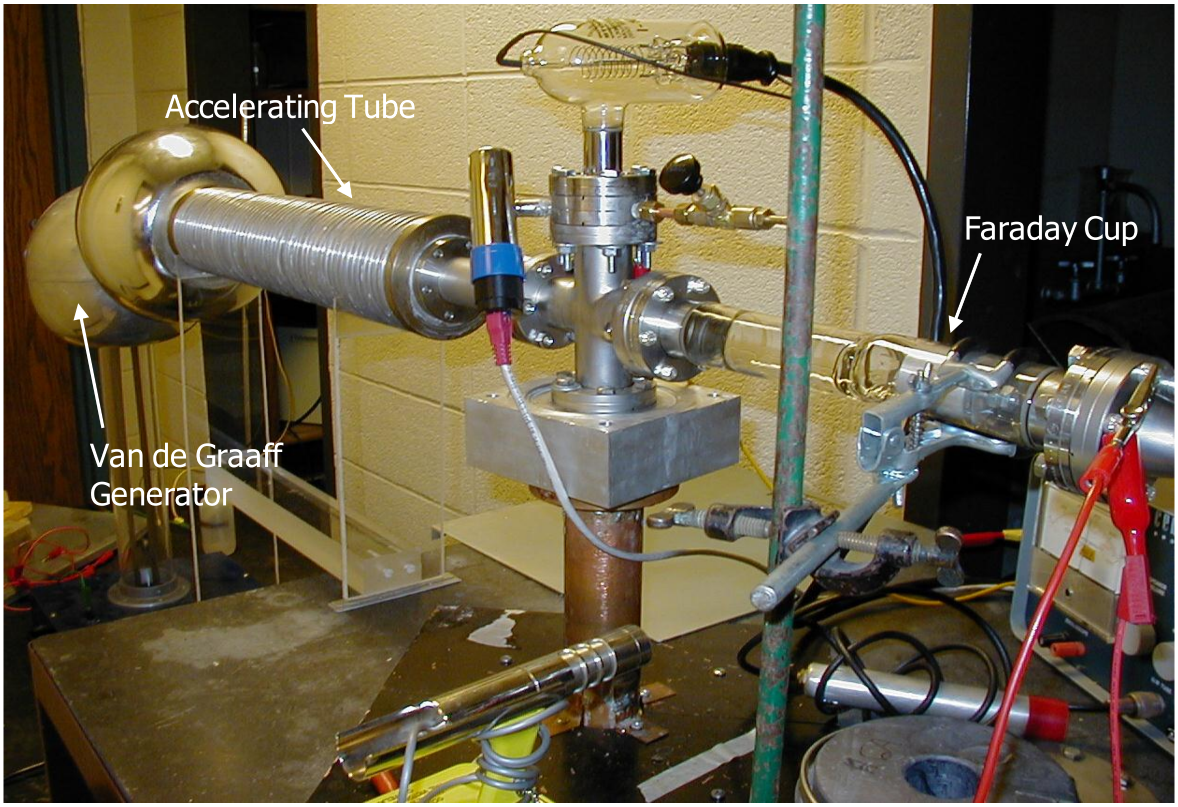

Figure 15. A photograph of the experimental setup with the Van de Graaff generator on the left, in contact with the high voltage terminal. The Faraday cup is visible inside the glass tube on the right.

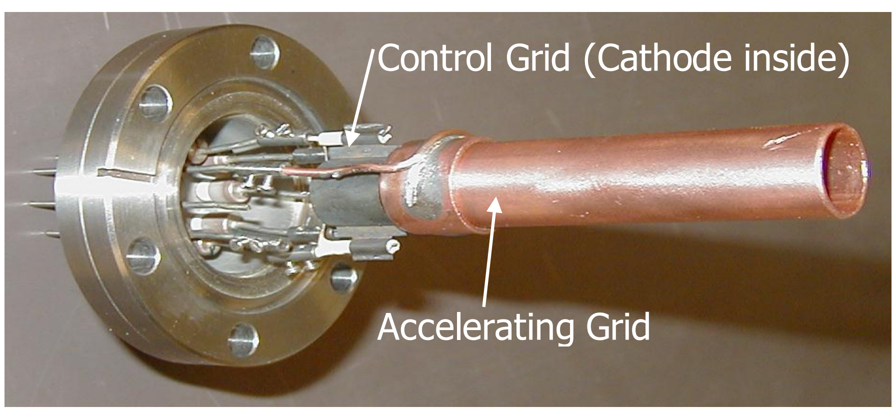

Figure 16. New electron gun design with 7.6 cm long copper pipe as the accelerating grid.

4.3 Results

When the filament was off and the high voltage was applied, there was no beam spot or beam current. There was no obvious discharges taking place from the high voltage terminal. Figure 17 is a photograph of the Faraday cup glowing during operation of the accelerator with the filament on. A sketch of the observed beam spot can be seen in Figure 18. The beam spot was stable but oddly shaped.

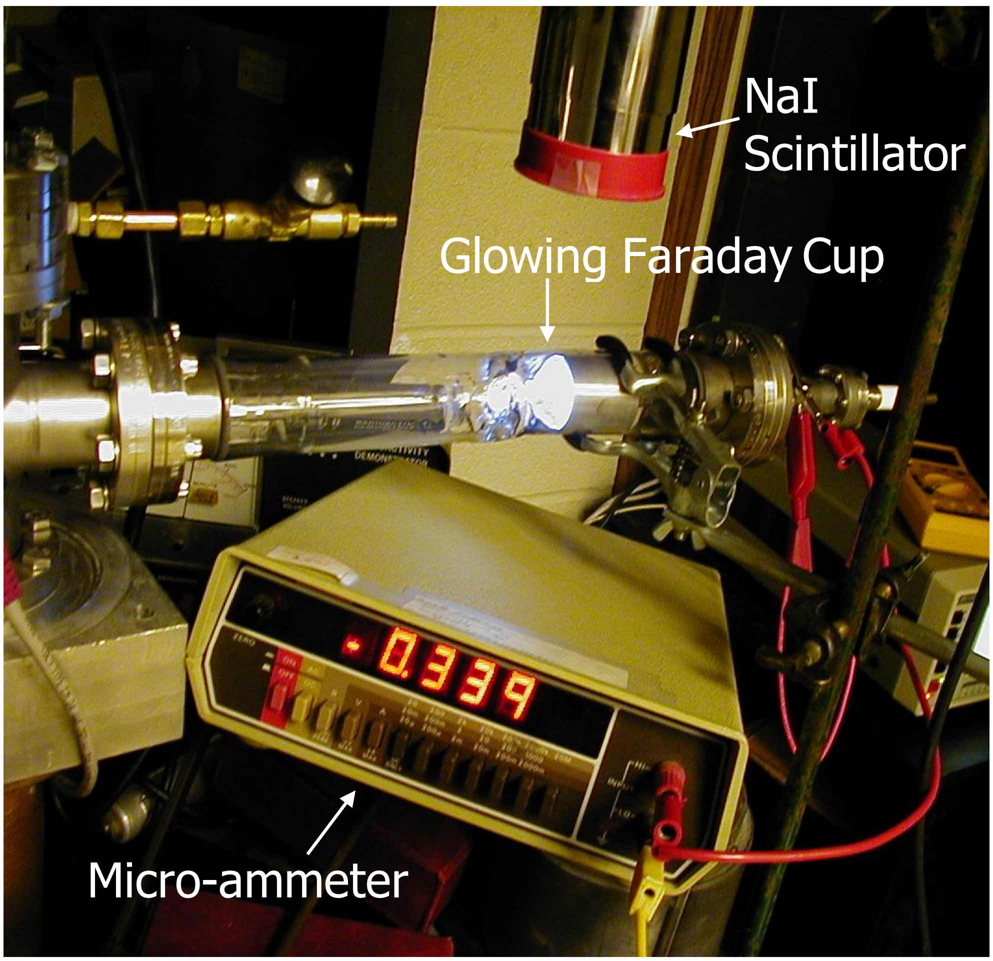

Figure 17. A photograph of the faraday cup during operation of the accelerator. The microammeter is reading beam current. A NaI scintillator was used to measure x-ray bremsstrahlung energy.

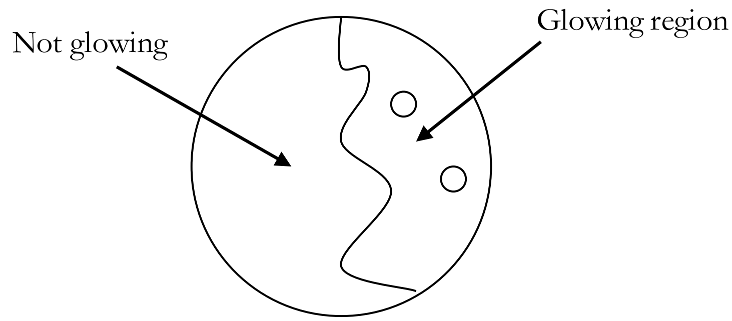

Figure 18. A very rough drawing of the beam spot with the glowing regions labeled. It is an odd shape.

Based on the Simion simulations, which demonstrated the lack of focusing, a well defined beam spot was not expected, but the very asymmetric odd shape was unexpected. The shape may be caused by the accelerating grid not being perfectly aligned with the axis of the accelerating tube. The Faraday cup was connected to ground through the ammeter shown. The average beam current was about 0.36 μA with maximum of approximately 0.4 μA. The NaI scintillator in the photograph was later placed outside the room a few feet away to measure the bremsstrahlung x-ray energy spectra, because pileup was occurring when the detector was so close to the Faraday cup.

The NaI detector used was a Bicron Coporation model 2M1/2 which has a crystal 2.54 cm thick and 5.1 cm in diameter. The NIM electronics diagram is shown in Figure 19. The NaI detector was connected to a photomultiplier tube at 900 V. The pulses from the photomultiplier tube were sent to an Ortec 113 pre-amplifier which was connected to a Tennelec TC 242 amplifier. The Amptek 8000A Multi Channel Analyzer digitized the pulse heights, which were read in the computer and histogrammed. The MCA was attached to the computer through an RS 232 serial cable.

The MCA must first be calibrated. To do this, radioactive sources which emit gamma radiation at known energies were placed by the detector until enough data had been collected to observe peaks in the energy spectrum. These corresponded to the known energy of the gamma rays from the sources. The energy of the peaks and their respective channel number were then used to determine a linear fit between the MCA channel and the energy. ^{22}Na, which emits gamma rays at 511 keV, and ^{133}Ba which emits gamma rays at 81 and 356 keV, were used for calibration (see Fig. 20).

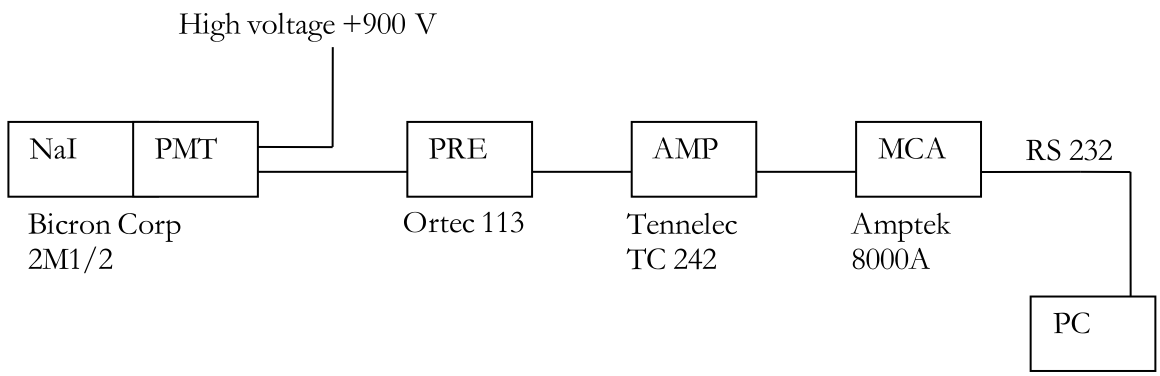

Figure 19. NIM electronics diagram of the setup used to measure the bremsstrahlung x-ray energy spectra. Pulses from the PMT travel to the pre-amplifier and the amplifier. They are then input to the computer by the MCA.

The energy of the bremsstrahlung x-rays is proportional to the energy the electrons lose when striking the Faraday cup. Therefore, the end point of the bremsstrahlung curve is where the electrons lose all their energy in striking the Faraday cup, which indicates the maximum energy of accelerator. From the bremsstrahlung energy curve in Figure 20 the energy of the accelerated electrons is in the vicinity of 180 keV. To obtain higher energies the belt speed on the Van de Graff could be increased. The beginning of the bremsstrahlung curve is probably cut off because low energy gamma rays did not make it through the door.

The radiation dosage rate was 10 mrem/hour approximately one foot from the faraday cup. A Victoreen Instrument Co. 6A calibrated survey meter was used to measure the radiation. The accelerator is located in room 105A in the science building. When the door between room 105A

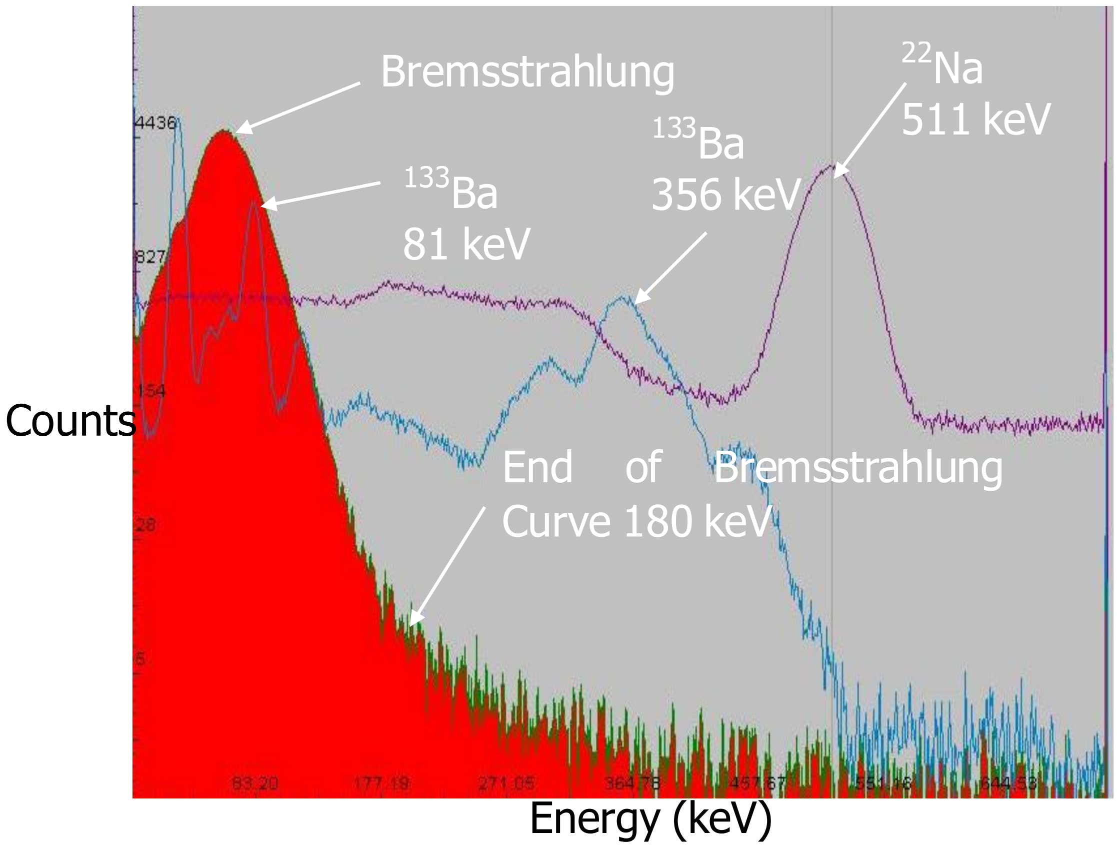

Figure 20. A plot of the bremsstrahlung x-ray energy spectra. ^{22}Na and ^{133}Ba sources were used for calibration. The end of the bremsstrahlung curve occurs somewhere around 180 keV.

and room 105 was closed, the radiation dosage rate right outside the door was 0.5 mrem/hour. The recommend dose limit for the average person is 100 mrem/year, thus, it would take 200 hours to reach this limit standing outside the door to the accelerator. It would take 10 hours to reach this limit standing next to the accelerator. For a radiation worker, the recommended dosage limit is 5 rem/year. It would take 10,000 hours (1.14 years) to reach this limit standing outside the dark room door in the lab (making it unatainable), and 500 hours if standing next to the accelerator. The radiation dosage rate at the door (closed) of room 105A leading to the hallway was less than 0.1 mrem/hour. The women's bathroom located next to the dark room received a dosage rate of less than 0.05 mrem/hour. The atrium to the science building received less than 0.05 mrem/hour. Outside the science building no radiation was detected. The kitchen of the faculty lounge, located directly above the darkroom received less than 0.1 mrem/hour.

Chapter 5

CONCLUSION

5.1 Summary

This thesis has described the design and construction of a small 200 keV electrostatic accelerator. The design was modeled with Simion 3D v7.0. The construction consisted of manufacturing 51 aluminum and 52 high density polyethylene rings on a CNC milling machine, and then gluing the rings together with vacuum epoxy. The accelerator was tested using a Van de Graaff generator in electrical contact with the high voltage terminal of the accelerator. Electrons from a modified electron gun were injected into the accelerator and accelerated toward a grounded Faraday cup where an oddly shaped beam spot was observed. Measurement of the bremsstrahlung x-ray energy spectrum indicates an electron beam energy in the vicinity of 180 keV. Higher energies may be obtained by turning up the belt speed on the Van de Graaff generator.

5.2 Plans for the Future

There are several plans for future modifications to the accelerator. As can be seen in Figure 17, the beam spot was not well focused. In the future something like the focusing grid in a CRT should be added to the electron gun in order to focus the beam onto the Faraday cup.

Another plan is to replace the electron with an ion source so a beam of positively charged ions could be produced. In an ion source, electrons (approximately 50 eV) are accelerated into a high pressure gas, ionizing it. The positive ions in the gas are then extracted with an electric field and injected into the accelerating tube [1]. An ion source can be used to create a beam of deuterons. Figure 21 is a plot of the cross section for the production of neutrons in the d-d reaction as a function of incident deuteron energy. The deuterons from this accelerator will have energies in the range of 150 keV. Taking advantage of the d-d reaction, deuterons can be accelerated into a deuterium impregnated target to create approximately 2.5 MeV neutrons. There are a variety of ways to obtain a deuterium impregnated target. If a thin copper target placed is placed in a deuterium beam, the copper will eventually become a deuterium impregnated target. However, the deuterium will be at different depths in the copper so the neutrons that are produced will have a span of energies.

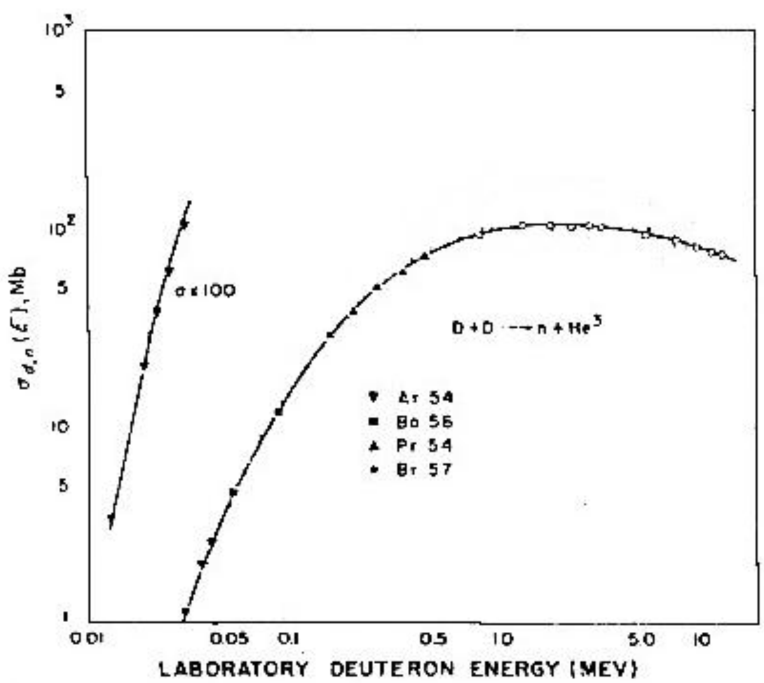

Figure 21. A plot showing the cross section for neutron production in the d-d reaction as a function of incident deuteron energy. Taken from reference [22].

Another way to obtain a deuterium target might be to use a thin film of D_2O ice formed using a liquid nitrogen "cold finger" arrangement. X-rays, an electron beam, positive ion beam, or neutron beam would then be available to perform experiments.

Vacuum System

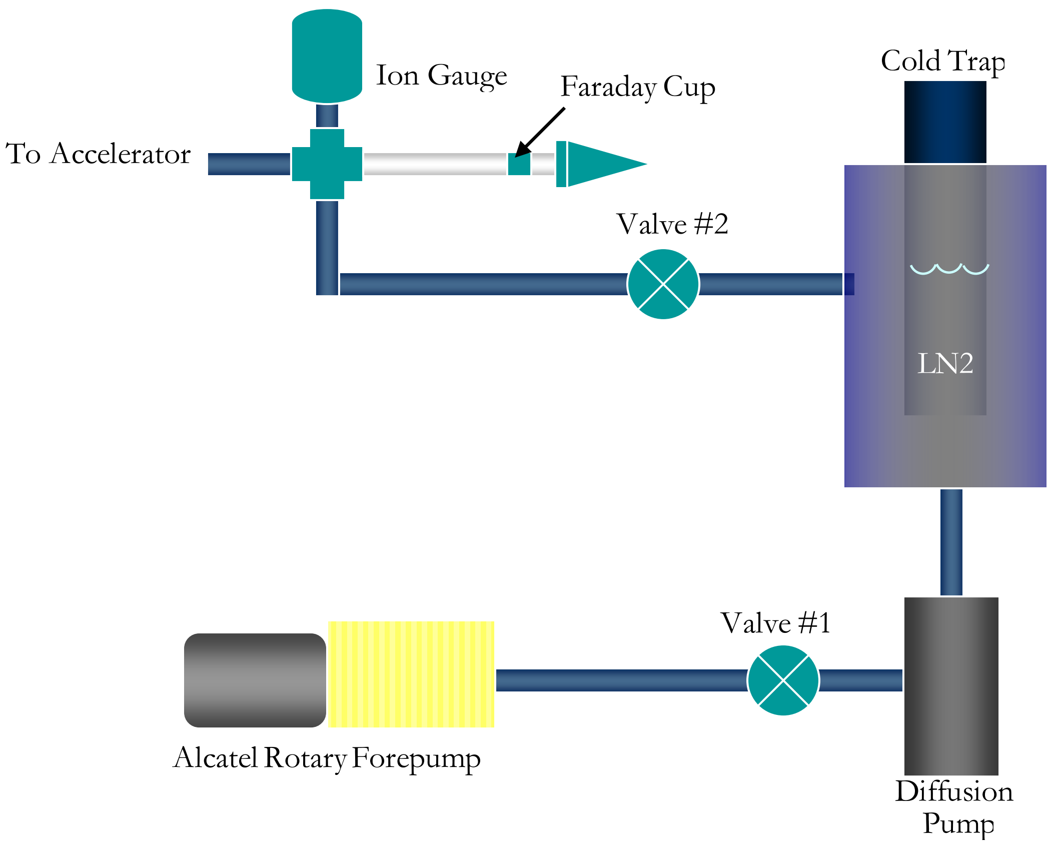

Figure 22. A simplified drawing of the vacuum system with the main parts labeled: rotary forepump, cold trap, and diffusion pump.

The vacuum system was used to evacuate the accelerating tube to approximately 1.5×10^{-5} Torr and is described in Ref. 19. The main components of the vacuum system are the rotary forepump, cold trap and diffusion pump as shown in Figure 22.

The Alcatel M2008A rotary forepump brings the pressure of the system down from atmospheric pressure to approximately 10^{-3} Torr. The forepump consists of a rotor turning off-center in a cylindrical stator with two spring loaded vanes running through the rotor as shown in Figure 23. Gas enters the pump through the inlet valve and is then compressed and forced through the exhaust valve as the rotor spins. Fisher Grand Maxima C (catalog no. 01-158-42) pump oil is used to maintain the seals in the forepump.

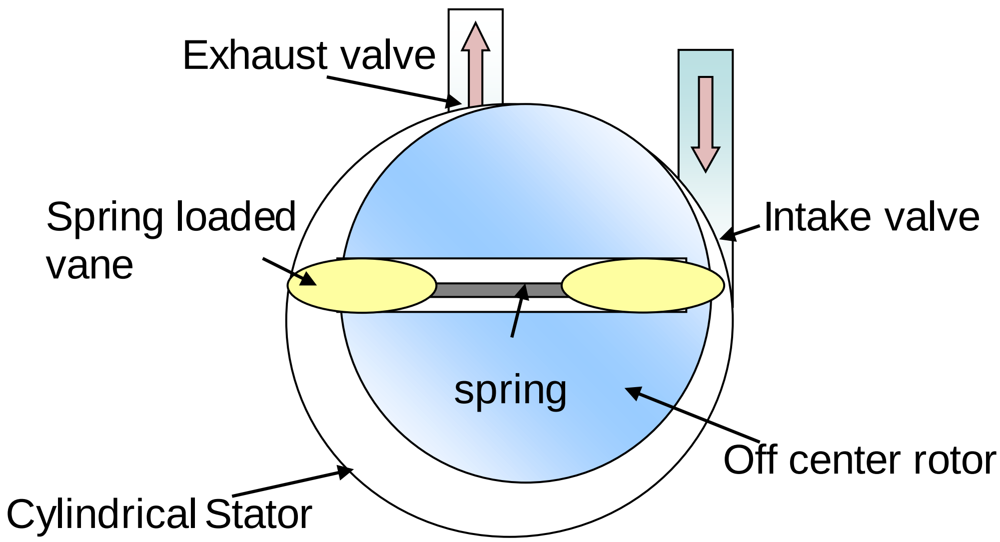

Figure 23. A simplified drawing of the rotary forepump. The off center rotor contains two spring loaded vanes and rotates in the cylindrical stator.

The cold trap was then filled with liquid nitrogen at 77 K. When air molecules moving through the vacuum system reach the vicinity of the cold trap, the low temperature causes the air molecules to lose most of their kinetic energy, so they are unable to overcome gravity and are drawn into the diffusion pump.

After the cold trap was filled, the diffusion pump was turned on. Current running through a heating element boils the oil in the bottom cup of the diffusion pump. The boiling oil is sprayed down toward the walls of the pump. A fan cools the pump which causes the oil vapor to condense and fall back down to the sump. The condensed oil traps air as it falls which is then taken out of the system by the forepump. This brought the pressure in the accelerating tube down to 1.5×10^{-5} Torr. The vapor pressure of the high density polyethylene rings may be 1.5×10^{-5} Torr, causing our system to never go below this pressure.

Figure 24 shows two photographs of the vacuum system. The forepump is visible in the foreground in (a) with the cold trap and diffusion pump in the background. In (b) the fan, which blows air over the cooling vanes of the diffusion pump, is visible as well as the diffusion pump and cold trap.

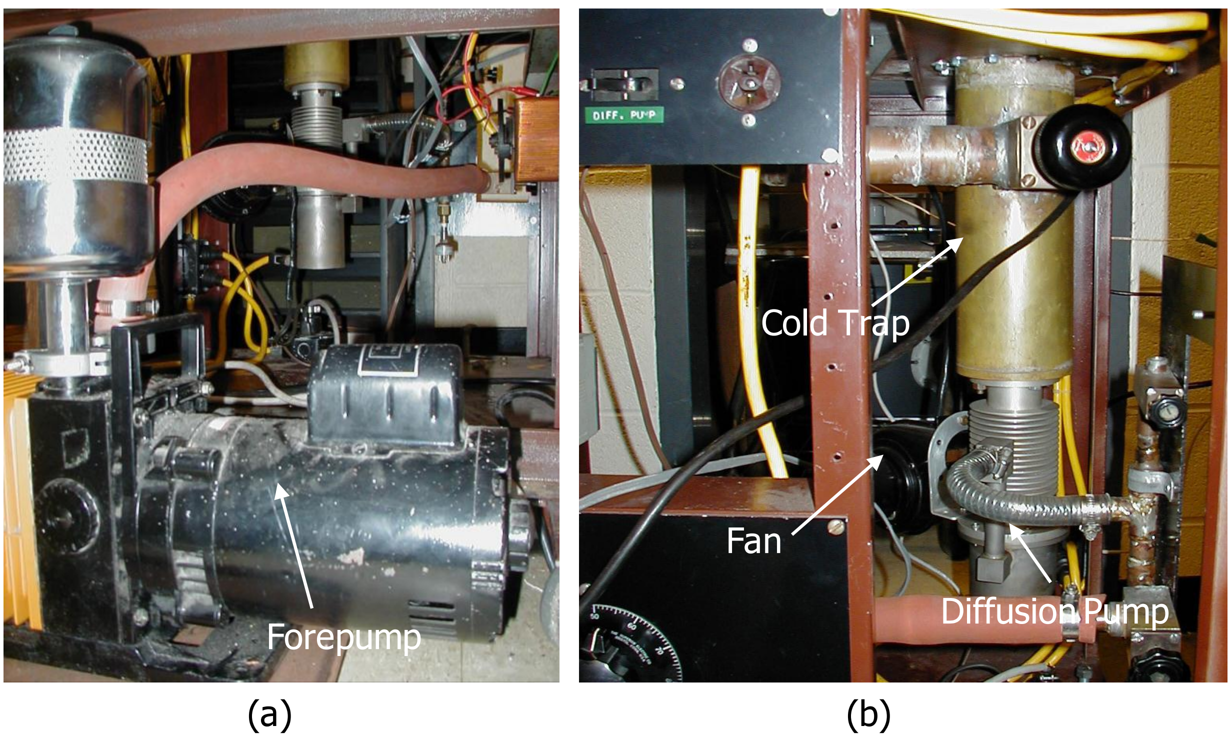

Figure 24. Photographs of the vacuum system with the main parts labeled.

A Granville-Phillips Helix Technology Convection Enhanced Pirani Gauge (catalog number 275071) was used to accurately measure pressures down to 10^{-3} Torr. Pressures below 10^{-4} Torr were measured using a Duniway Stockroom I-100-K Glass Tabulated Ion Gauge. Data from the gauges were monitored with a Stanford Research Center IGC 100 Ion Gauge Controller.

Appendix B

Interlock System

An interlock system was designed to provide a safety mechanism against the accelerator being turned on while a person is in the room. A circuit diagram is of the system [23] is shown in Figure 26 . The controller box is mounted to the wall outside the dark room. A key must be turned and switch flipped to turn the system on. The doors are wired to magnetic switches which will not allow the Van de Graaff generator to be turned on if a door is open and shut the Van de Graaff generator off if a door is opened during operation. There is also a large red emergency stop button on the wall inside the dark room which shuts off the accelerator if pushed. For the accelerator to be turned back on, the emergency stop button must be reset and a key must be turned on the controller box to reset the system.

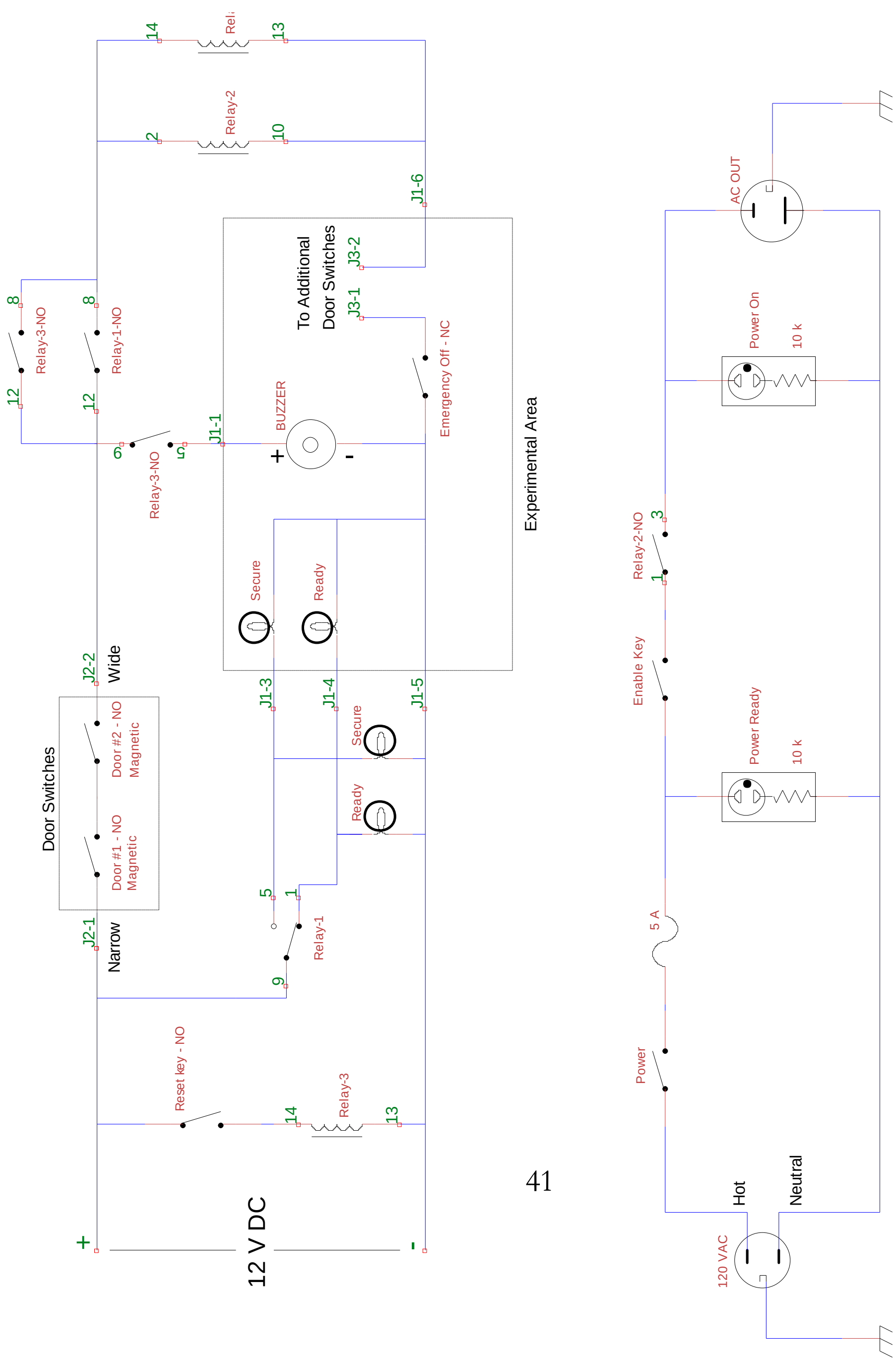

Figure 26. Circuit diagram of

Appendix C

CNC MILLING MACHINE

C.1 Milling Machine

A Sherline Products model 5400-CNC mill was used to make the rings for the accelerator. The stepper motors on the mill were manufactured by the Micro Kinetics Corporation. Two model 23M80D's stepper motors were used for x-y axis control. A model 23M1102 stepper motor controlled the z-axis. The Micro Kinetics Corp. program Mill Master Pro V 1.7 was installed on a 486 computer with 20 MB ram to interface with the Micro Kinetics Optistep Plus controller inside the Might Drive model 3600-503 to control the mill.

During this project the threads on brass saddle nut on the x and y axis would repeatedly get shredded causing those axes to stop working at inopportune times, breaking many end mills. This machine was not designed to handle the workload it was subjected to and it is recommended that a much more durable machine be used in projects of this magnitude in the future.

C.2 Computer Code for High Density Polyethylene Rings

The following is a brief synopsis of the commands used in the computer code.

G91: Puts machine in incremental programming mode (all distances are measured relative to the tools current position).
G75: Sets the multiple arc programming mode, enabling machine to cut circles.
G00: Quick move along specified direction(s).
M03: Sets spindle motor spinning clockwise.
G01: Cuts specified distance along specified axis.
G02 J - *a*: Cuts a circle of radius a clockwise with the tool's current location as the top of the circle.
M25: Returns tool to starting position (z-axis is done first).
M05: Shuts spindle motor off.
FXX: Sets the feed rate of the axis to XX.

The following code was used to cut the high density polyethylene rings.

```
/   {fixture}: CLAMPS   {Units}: INCH
/   {SLENGTH}: 5.5000   {SWIDTH}: 5.5000   {SHEIGHT}: 0.2700
/   {X Start}: 0        {Y Start}: 0       {Z Start}: 0.05
/   {X Origin Zero}: 1  {Y Origin Zero}: -1  {Z Origin Zero}: -1
G91
G75
G00 X2.75 Y-.3975 /TOP OF TOP CIRCLE
M03
G01         Z-.104  F30
G02              J-.065
G01         Z-.054
G02              J-.065
G01         Z-.054
G02              J-.065
G01         Z-.054
G02              J-.065
G01         Z-.054
G02              J-.065
G00         Z.32
G00 Y-2.8        /TOP OF BOTTOM CIRCLE
G01         Z-.104
G02              J-.065
G01         Z-.054
G02              J-.065
G01         Z-.054
G02              J-.065
G01         Z-.054
G02              J-.065
G01         Z-.054
G02              J-.065
G00         Z.32
G00 Y2.2725      /TOP OF MIDDLE HOLE
G01         Z-.104
G02              J-.9375
G01         Z-.054
G02              J-.9375
G01         Z-.054
G02              J-.9375
G01         Z-.054
G02              J-.9375
```

```
G01          Z-.054
G02              J-.9375
G00          Z.32
G00 X-1.4 Y-.8725   /TOP OF LEFT CIRCLE
G01          Z-.104
G02              J-.065
G01          Z-.054
G02              J-.065
G01          Z-.054
G02              J-.065
G01          Z-.054
G02              J-.065
G01          Z-.054
G02              J-.065
G00          Z.32
G00 X2.8         /TOP OF RIGHT CIRCLE
G01          Z-.104
G02              J-.065
G01          Z-.054
G02              J-.065
G01          Z-.054
G02              J-.065
G01          Z-.054
G02              J-.065
G01          Z-.054
G02              J-.065
G00          Z.32
G00 X-1.4 Y1.7975 /TOP OF RING
G01          Z-.104
G02              J-1.8625
G01          Z-.054
G02              J-1.8625
G01          Z-.054
G02              J-1.8625
G01          Z-.054
G02              J-1.8625
G01          Z-.054
G02              J-1.8625
G00          Z.34
M25
M05            /END OF PROGRAM
```

C.3 Computer Code for Aluminum Rings

The following code was used to cut the aluminum rings.

```
/   {fixture}: CLAMPS   {Units}: INCH
/   {SLENGTH}: 5.5000   {SWIDTH}: 5.5000   {SHEIGHT}: 0.1400
/   {X Start}: 0        {Y Start}: 0       {Z Start}: 0.05
/   {X Origin Zero}: 1  {Y Origin Zero}: -1  {Z Origin Zero}: -1
G91
G75
G00  X2.75  Y-.5975 /TOP OF TOP CIRCLE
M03
F05
G01         Z-.06
F30
G02              J-.065
F01
G01         Z-.01
F30
G02              J-.065
F01
G01         Z-.01
F30
G02              J-.065
F01
G01         Z-.01
F30
G02              J-.065
F01
G01         Z-.01
F30
G02              J-.065
F01
G01         Z-.01
F30
G02              J-.065
F01
G01         Z-.01
F30
G02              J-.065
F01
G01         Z-.01
```

```
F30
G02           J-.065
F01
G01       Z-.01
F30
G02           J-.065
F01
G01       Z-.01
F30
G02           J-.065
F01
G01       Z-.01
F30
G02           J-.065
F01
G01       Z-.01
F30
G02           J-.065
F01
G01       Z-.01
F30
G02           J-.065
F01
G01       Z-.01
F30
G02           J-.065
G00       Z.19
G00  Y-2.8     /TOP OF BOTTOM CIRCLE
F05
G01       Z-.06
F30
G02           J-.065
F01
G01       Z-.01
F30
G02           J-.065
F01
G01       Z-.01
F30
G02           J-.065
F01
G01       Z-.01
```

```
F30
G02        J-.065
F01
G01     Z-.01
F30
G02        J-.065
F01
G01     Z-.01
F30
G02        J-.065
F01
G01     Z-.01
F30
G02        J-.065
F01
G01     Z-.01
F30
G02        J-.065
F01
G01     Z-.01
F30
G02        J-.065
F01
G01     Z-.01
F30
G02        J-.065
F01
G01     Z-.01
F30
G02        J-.065
F01
G01     Z-.01
F30
G02        J-.065
F01
G01     Z-.01
F30
G02        J-.065
F01
G01     Z-.01
F30
G02        J-.065
```

```
G00          Z.19
G00 Y2.025       /TOP OF MIDDLE HOLE
F05
G01          Z-.06
F30
G02              J-.6875
F01
G01          Z-.01
F30
G02              J-.6875
F01
G01          Z-.01
F30
G02              J-.6875
F01
G01          Z-.01
F30
G02              J-.6875
F01
G01          Z-.01
F30
G02              J-.6875
F01
G01          Z-.01
F30
G02              J-.6875
F01
G01          Z-.01
F30
G02              J-.6875
F01
G01          Z-.01
F30
G02              J-.6875
F01
G01          Z-.01
F30
G02              J-.6875
F01
G01          Z-.01
F30
G02              J-.6875
```

```
F01
G01       Z-.01
F30
G02            J-.6875
F01
G01       Z-.01
F30
G02            J-.6875
F01
G01       Z-.01
F30
G02            J-.6875
F01
G01       Z-.01
F30
G02            J-.6875
G00       Z.19
G00  X-1.4  Y-.6225    /TOP OF LEFT CIRCLE
F05
G01       Z-.06
F30
G02            J-.065
F01
G01       Z-.01
F30
G02            J-.065
F01
G01       Z-.01
F30
G02            J-.065
F01
G01       Z-.01
F30
G02            J-.065
F01
G01       Z-.01
F30
G02            J-.065
F01
G01       Z-.01
F30
G02            J-.065
```

```
F01
G01        Z-.01
F30
G02            J-.065
F01
G01        Z-.01
F30
G02            J-.065
F01
G01        Z-.01
F30
G02            J-.065
F01
G01        Z-.01
F30
G02            J-.065
F01
G01        Z-.01
F30
G02            J-.065
F01
G01        Z-.01
F30
G02            J-.065
F01
G01        Z-.01
F30
G02            J-.065
F01
G01        Z-.01
F30
G02            J-.065
G00        Z.19
G00 X2.8       /TOP OF RIGHT CIRCLE
F05
G01        Z-.06
F30
G02            J-.065
F01
G01        Z-.01
F30
G02            J-.065
```

```
F01
G01           Z-.01
F30
G02                J-.065
F01
G01           Z-.01
F30
G02                J-.065
F01
G01           Z-.01
F30
G02                J-.065
F01
G01           Z-.01
F30
G02                J-.065
F01
G01           Z-.01
F30
G02                J-.065
F01
G01           Z-.01
F30
G02                J-.065
F01
G01           Z-.01
F30
G02                J-.065
F01
G01           Z-.01
F30
G02                J-.065
F01
G01           Z-.01
F30
G02                J-.065
F01
G01           Z-.01
F30
G02                J-.065
F01
G01           Z-.01
```

```
F30
G02            J-.065
F01
G01        Z-.01
F30
G02            J-.065
G00        Z.19
G00  X-1.4 Y1.9975      /TOP OF RING
F05
G01        Z-.06
F30
G02            J-2.0625
F01
G01        Z-.01
F30
G02            J-2.0625
F01
G01        Z-.01
F30
G02            J-2.0625
F01
G01        Z-.01
F30
G02            J-2.0625
F01
G01        Z-.01
F30
G02            J-2.0625
F01
G01        Z-.01
F30
G02            J-2.0625
F01
G01        Z-.01
F30
G02            J-2.0625
F01
G01        Z-.01
F30
G02            J-2.0625
F01
G01        Z-.01
```

```
F30
G02          J-2.0625
F01
G01     Z-.01
F30
G02          J-2.0625
F01
G01     Z-.01
F30
G02          J-2.0625
F01
G01     Z-.01
F30
G02          J-2.0625
F01
G01     Z-.01
F30
G02          J-2.0625
F01
G01     Z-.01
F30
G02          J-2.0625
G00     Z.2
M25
M05        /END OF PROGRAM
```

References

[1] J.Blewett, M. Livingston. **Particle Accerators** (McGraw-Hill, New York, 1962).

[2] Vollrath, *Phys. Rev.*, **42**: 298 (1932).

[3] E. Rutherford, *The London, Edinburgh and Dublin Philosophical Magazine and Journal of Science*, 6th series, **37**: 581 (1919).

[4] E. Rutherford, *Proc. Roy. Soc.* (London), **117**: 300 (1927).

[5] G. Breit, M.A. Tuve, and O.Dahl, *Phys. Rev.*, **35**: 51 (1930).

[6] M.A. Tuve, G. Breit, and L.R. Hafstad, *Phys. Rev.*, **35**: 66 (1930).

[7] M.A. Tuve, L.R. Hafstad, O. Dahl, *Phys. Rev.*, **35**: 1406 (1930), **36**: 1261 (1930).

[8] J.D. Cockroft and E.T.S Walton, *Proc. Roy. Soc.* (London), **A136**: 619(1932); **A137**: 229(1932); **A144**: 704(1934).

[9] R.J. Van de Graaff, *Phys. Rev*, **38**: 1919A (1931).

[10] R. J. Van de Graaff *et. al.*, *Phys. Rev*, **43**: 149 (1933).

[11] R. J. Van de Graaff *et. al.*, *Phys. Rev.*, **49:** 761 (1936).

[12] H. H. Barshcall, "Electrostatic Accelerators" **The Physics Teacher**, September 1970, 316.

[13] Boston Museum of Science "The History of the Van de Graaff Generator". http://www.mos.org/sln/toe/history.html. April 22, 2004

[14] E. O. Lawrence and M. S. Livingston, *Phys. Rev.*, **40**: 19 (1932).

[15] "FermiLab". http://ww.fnal.gov. April 28, 2004.

[16] C.L. Stong. "A Homemade Atom Smasher". **Scientific American**, Vol. 200, no. 1, January 1959.

[17] C.L. Stong. "How to Build a Machine to Produce Low-Energy Protons and Deuterons". **Scientific American**, Vol. 225, no. 2, August 1971.

[18] F. M. Niell (personal communicatoin) 2003 (see "Fred's World of Science: Linear Accelerator"

http://www-personal.umich.edu/~mrniell/linac.html. April 19, 2004.)

[19] B. Winey, B.S. thesis, Houghton College, 2002.

[20] R.J. Van de Graaff, *Physical Society Progress Reports*, Vol **XI** (1948).

[21] David A. Dahl. **Simion 3D Version 7.0 User's Manual** (Bechtel Bwxt Idaho, LLC, 2000).

[22] J. E. Brolley, Jr. and J.L. Fowler in **Interscience Monographs and Texts in Physics and Astronomy Vol IV: Fast Neutron Physics**, edited by R.E. Marshak (Interscience Publishers, Inc., NY, 1960)

[23] M. Yuly (private communication) February 2004.